

RSC Advances



This is an *Accepted Manuscript*, which has been through the Royal Society of Chemistry peer review process and has been accepted for publication.

Accepted Manuscripts are published online shortly after acceptance, before technical editing, formatting and proof reading. Using this free service, authors can make their results available to the community, in citable form, before we publish the edited article. This *Accepted Manuscript* will be replaced by the edited, formatted and paginated article as soon as this is available.

You can find more information about *Accepted Manuscripts* in the [Information for Authors](#).

Please note that technical editing may introduce minor changes to the text and/or graphics, which may alter content. The journal's standard [Terms & Conditions](#) and the [Ethical guidelines](#) still apply. In no event shall the Royal Society of Chemistry be held responsible for any errors or omissions in this *Accepted Manuscript* or any consequences arising from the use of any information it contains.

Self-supported construction of 3D CdMoO₄ hierarchical structures from nanoplates with enhanced photocatalytic properties

Wenshou Wang,^{a,b,c} Jianxun Cui,^a Panpan Wang,^a Liang Zhen,^{*a,c} Wenzhu Shao,^a and Zhonglin Chen^b

^aSchool of Materials Science and Engineering, Harbin Institute of Technology, Harbin 150001, China.

^bState Key Laboratory of Urban Water Resources and Environment, School of Municipal & Environmental Engineering, Harbin Institute of Technology, Harbin 150090, China.

^cMOE Key Laboratory of Micro-systems and Micro-structures Manufacturing, Harbin Institute of Technology, Harbin 150080, China

* Corresponding author. Tel: +86-451-86412133; Fax: +86-451-86413922; E-mail: lzhen@hit.edu.cn

Abstract: Three-dimensional (3D) CdMoO₄ hierarchical structures constructed by single-crystalline nanoplates were prepared by a facile hydrothermal route. The obtained samples were systematically characterized by X-ray powder diffraction (XRD), scanning electron microscopy (SEM), transmission electron microscopy (TEM) and UV-Vis spectrophotometer. The morphology modulation of the as-prepared products could be easily tuned by changing the concentration of reactants, reaction temperature, molybdenum source, pH value and reaction time. The formation process of CdMoO₄ hierarchical structures was related to the two-step growth, in which CdMoO₄ main nanoplates were formed first in the synthesis, followed by self-construction of small nanoplates on both side of the main nanoplates in a regular fashion. The photocatalytic activities of CdMoO₄ hierarchical structures and nanoplates for degradation of Rhodamine B (RhB) under ultraviolet (UV) light irradiation were also evaluated. CdMoO₄ hierarchical structures constructed by nanoplates have a higher photocatalytic activity toward photo-degradation of RhB than that of CdMoO₄ nanoplates, mainly due to their unique morphology and high crystallinity.

1. Introduction

Hierarchical inorganic micro-/nanostructures assembled from one-dimensional (1D) and two-dimensional (2D) nano-building blocks have received increasing attentions in recent years because they improve the physical and chemical properties of the nanoscale materials with simple configurations.¹⁻⁴ The surfactant-assisted hydrothermal

method is widely used to achieve various inorganic hierarchical structures, in which surfactants act as directing agents for hierarchical structures.⁵⁻⁷ However, the introducing of organic additives greatly increase the complexity of a synthetic procedure and inevitably introduce heterogeneous impurities in the products. In addition, although great progress has been made on the synthesis of 3D hierarchical structures, the materials are mainly limited to metals,^{8,9} binary metal oxides^{10,11} and sulfides.^{12,13} Therefore, it is still of fundamental significance to develop a convenient and effective approach for the synthesis of ternary metal oxides with 3D hierarchical structures.

Among various metal molybdates, CdMoO_4 is an important metal molybdate, which has stimulated great interest due to its electronic excitation at VUV synchrotron radiation¹⁴ and pressure-induced phase transformations.¹⁵ In addition, as a wide band gap semiconductor of 3.25 eV, CdMoO_4 is expected to be a photocatalyst under ultraviolet (UV) radiation.¹⁶ A few efforts have been devoted recently to the synthesis of CdMoO_4 micro-/nanostructures via various approaches. For example, we have developed a general room temperature aqueous solution route for the preparation of CdMoO_4 hollow,¹⁷ core-shell microspheres,¹⁸ and mesoporous hollow nanospheres.¹⁹ CdMoO_4 micro-/nanostructures with different shapes, such as spheres,²⁰ octahedrons,²¹ nanorods,²² cake,²³ and nanoplates,²⁴ were prepared by hydrothermal and microemulsion-mediated methods. However, compared with other metal molybdates, the synthesis and properties study of CdMoO_4 have been lagging far behind. There have been rare examples focusing on the synthesis of 3D CdMoO_4 hierarchical structures constructed from nanoplates, although it is expected that the specific structures would exhibit better photocatalytic activity because they are more structurally stable and can provide more reaction centers than 2D nanoplates.²⁵ Herein, we report a facile hydrothermal method for the construction of 3D CdMoO_4 hierarchical structures from nanoplate building blocks. The effects of experimental conditions including concentration of reactants, reaction temperature, Mo source, pH value and reaction time on the morphology and size of CdMoO_4 microstructures have been investigated systematically. An interesting structural evolution from 2D CdMoO_4 nanoplates to 3D hierarchical structures composed of nanoplates was observed based on increasing concentrations of reaction precursors. The two-step growth is proposed for the 3D

CdMoO₄ hierarchical structures, in which CdMoO₄ main nanoplates were formed first in the synthesis, followed by self-construction of small nanoplates on both side of the main nanoplates in a regular fashion. In addition, the photocatalytic activity of the obtained samples were studied. The as-obtained 3D CdMoO₄ hierarchical structures have a higher photocatalytic activity toward photo-degradation of RhB than that of CdMoO₄ nanoplates.

2. Experimental section

All reagents were analytical grade and used as received without further purification. In a typical synthesis process, 25 mL of CdCl₂ aqueous solution (0.2 M) was added into 25 mL of mixed aqueous solutions of (NH₄)₆Mo₇O₂₄ (0.044 M) and NaCl (0.8 M) in a glass beaker at room temperature under magnetic stirring. The initial pH value is ~ 5. After stirring for 10 min, the final mixture was directly transferred into a 50 ml Teflon-lined stainless autoclave, filled up to 80% of its capacity. The autoclave was maintained at 200 °C for 2h in an electrical oven and then air-cooled to room temperature. The precipitate was collected, filtered off and washed with distilled water and absolute ethanol several times. After drying in air at 60 °C for 6h, the final powders were obtained. During the synthesis, the molar ratio among (NH₄)₆Mo₇O₂₄, NaCl and CdCl₂ were fixed as typical synthesis when the concentrations of reagents were changed.

X-ray diffraction pattern (XRD) was obtained on a Rigaku D/max-rA X-ray diffractometer with Cu K α radiation ($\lambda = 1.5406 \text{ \AA}$). The morphology of the samples was observed by scanning electron microscopy (SEM), performed on FEI-Quanta 200F scanning electron microscopy. The transmission electron microscopy (TEM) and selected area electron diffraction (SAED) pattern were taken out on a Phillips Tecnai 20 microscopy with an accelerating voltage of 200 kV. The optical diffuse reflectance spectrum was measured on a UV-Vis scanning spectrophotometer (SHIMADZU UV 2550). Nitrogen adsorption isotherms were obtained at 77 K using a nitrogen sorption instrument (Quantachrome NOVA 4200e).

The photocatalytic activities of the samples were evaluated by the RhB decomposition under UV illumination. UV light was obtained by a 10W UV lamp at room temperature ($\lambda = 254 \text{ nm}$, GPH212T5L/4, Germany). It was surrounded by a quartz jacket to cut-off any radiation with wavelength below 254 nm. The suspension temperature was $20 \pm 2^\circ\text{C}$ for all the runs. For the photocatalytic test, aqueous solutions (usually 400

mL) of RhB (1.0×10^{-5} M) and CdMoO_4 powder ($0.5 \text{ g}\cdot\text{L}^{-1}$) were placed in a vessel. Prior to illumination, the suspensions were magnetically stirred in dark for about 10 min to ensure the adsorption/desorption equilibrium. The suspensions were kept under constant air-equilibrated conditions with magnetic stirring before and at given time intervals. At given time intervals, 5 mL aliquots were samples, and centrifuged to remove CdMoO_4 particles. The filtrates were analyzed on a UV-Vis spectrometer (Schimadzu UV2550) by monitoring the characteristic absorption of RhB at $\lambda = 553 \text{ nm}$ to evaluate the photocatalytic degradation process.

3. Results and discussion

The 3D CdMoO_4 hierarchical structures are successfully obtained through the hydrothermal reaction at 200°C between CdCl_2 and $(\text{NH}_4)_6\text{Mo}_7\text{O}_{24}$. The SEM images of the products obtained with different precursors' concentrations are shown in Fig. 1. With low concentration of CdCl_2 aqueous solution at 0.02 M, the products are hierarchical structures, constructed by one main nanoplate with length of $\sim 3 \mu\text{m}$ and thickness of $\sim 200 \text{ nm}$, and some small nanoplates on both surface of the main nanoplate (Fig. 1a-c). Higher magnification SEM images reveal that the small nanoplates with several hundreds nanometers are embedded on the surface of the main nanoplates along the fringe, tending to form hierarchical structures. Increasing the concentration of CdCl_2 aqueous solution to 0.04 M, CdMoO_4 hierarchical structures with uniform morphology are prepared (Fig. 1d). The size of hierarchical structures increases to $\sim 4 \mu\text{m}$ while the thickness of main nanoplates is still $\sim 200 \text{ nm}$. More nanoplates are constructed on the main nanoplates with a layer-by-layer behavior, as shown in Fig. 1e. Side view of an individual hierarchical structure further demonstrates that the small nanoplates grow on both sides of the main nanoplate (Fig. 1f). A typical EDS spectrum of the CdMoO_4 hierarchical structures shows strong peaks from Cd, Mo and O, giving a stoichiometric composition of CdMoO_4 (Fig. S1). Further increasing the concentration of CdCl_2 aqueous solution to 0.2 M produces a uniform population of hierarchical structures with an interesting doughnut shape—flattened spheres each containing a concavity on its surface, as shown in Fig. 1g. The size of hierarchical structures further increase to $\sim 6 \mu\text{m}$. SEM images shown in Fig. 1h and 1i reveals that each doughnut is composed of many layers of nanoscale plate-like structures. These nanoplates are

arranged at progressively increasing angles to the radial axis and are highly directed to form arrays in a regular fashion. The morphologies evolution dependent on precursors' concentration indicates that CdMoO_4 main nanoplates are formed first in the synthesis, followed by self-construction of small nanoplates on both side of the main nanoplates in a regular fashion.

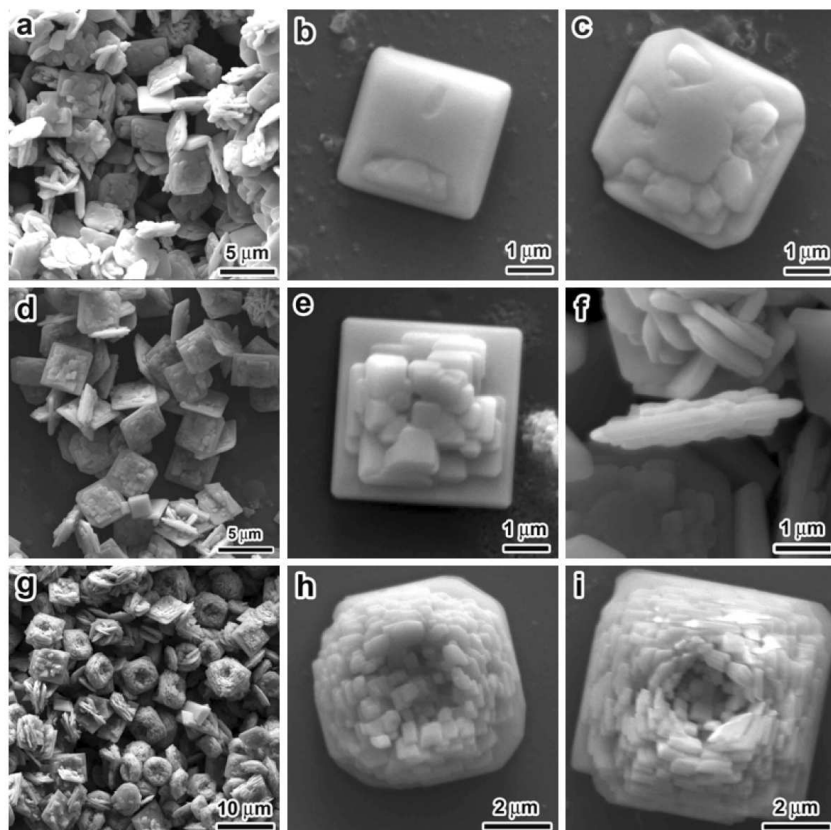


Fig. 1. SEM images of CdMoO_4 samples obtained at 200 °C with different concentrations of CdCl_2 aqueous solution. (a-c) 0.02 M, (d-f) 0.04 M and (g-i) 0.2 M.

Fig. 2 shows the XRD pattern of the 3D CdMoO_4 hierarchical structures prepared with different precursors' concentration. All of the observed diffraction peaks can be perfectly indexed to those of tetragonal phase of CdMoO_4 (JCPDS 07-0209). The strong and sharp diffraction peaks indicate good crystallinity in the as-synthesized products. No peaks of other impurity phases are detected in this pattern, suggesting that CdMoO_4 products with high phase-purity can be easily obtained by this synthesis.

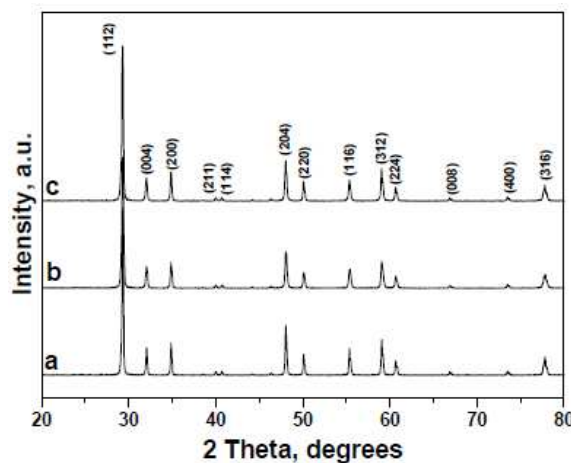


Fig. 2. XRD patterns CdMoO₄ samples obtained at 200 °C with different concentrations of CdCl₂ aqueous solution. (a-c) 0.02 M, (d-f) 0.04 M and (g-i) 0.2 M.

Fig. 3a shows a typical TEM image of CdMoO₄ hierarchical structure obtained with concentration of CdCl₂ aqueous solution at 0.02 M, which is consistent with SEM images shown in **Fig. 1b** and **1c**. The SAED pattern recorded on the plate is indexed as [010] zone axes, revealing its single crystalline in nature (**Fig. 3b**). The TEM image of CdMoO₄ hierarchical structure obtained with concentration of CdCl₂ aqueous solution at 0.2 M is shown in **Fig. 3c**, in which the contrast at the center of the particles is lower than that of the edges, confirming the doughnut structures. SAED pattern recorded on the edge of the doughnuts also indicates its single crystalline with [010] zone axes (**Fig. 3d**).

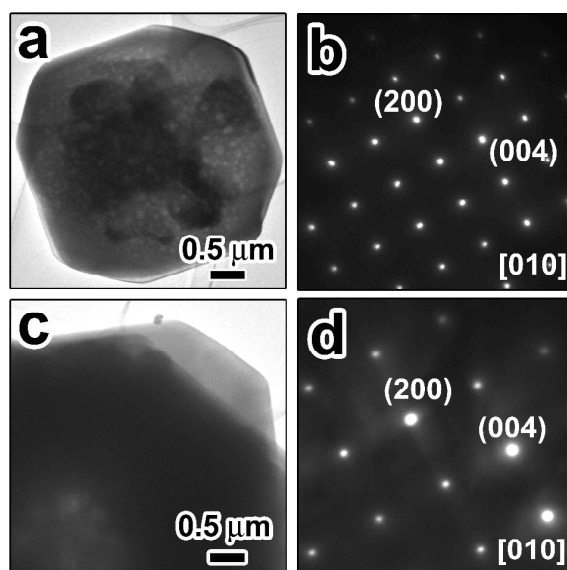


Figure 3. TEM images (a, c) and SAED patterns (b, d) of the CdMoO₄ hierarchical structures.

The concentration-dependent change of morphology of CdMoO_4 samples from nanoplates to hierarchical structures is further demonstrated at low reaction temperature. Fig. 4 shows the SEM images of CdMoO_4 samples prepared at 100°C with different precursors' concentrations. All samples have a very uniform shape. At this low reaction temperature, CdMoO_4 main nanoplates are still formed first and followed by self-construction of small nanoplates on both side of the main nanoplates to form CdMoO_4 hierarchical structures upon increasing the precursors' concentrations. However, the size of the CdMoO_4 hierarchical structures is small and the thickness of main nanoplates is thin compared with the samples prepared at 200°C while keeping other reaction conditions the same. The similar morphology evolution is also observed at reaction temperature of 150°C , as shown in Fig. 5. The concentration-dependent change of morphology of CdMoO_4 samples at reaction temperature of 100 , 150 and 200°C demonstrate the synthesis reaction is very sensitive to precursor's concentration and reaction temperature. Both high concentration of precursors and reaction temperature promote the self-construction of nanoplates on the initial formed main nanoplates, resulting in the formation of CdMoO_4 hierarchical structures with large sizes.

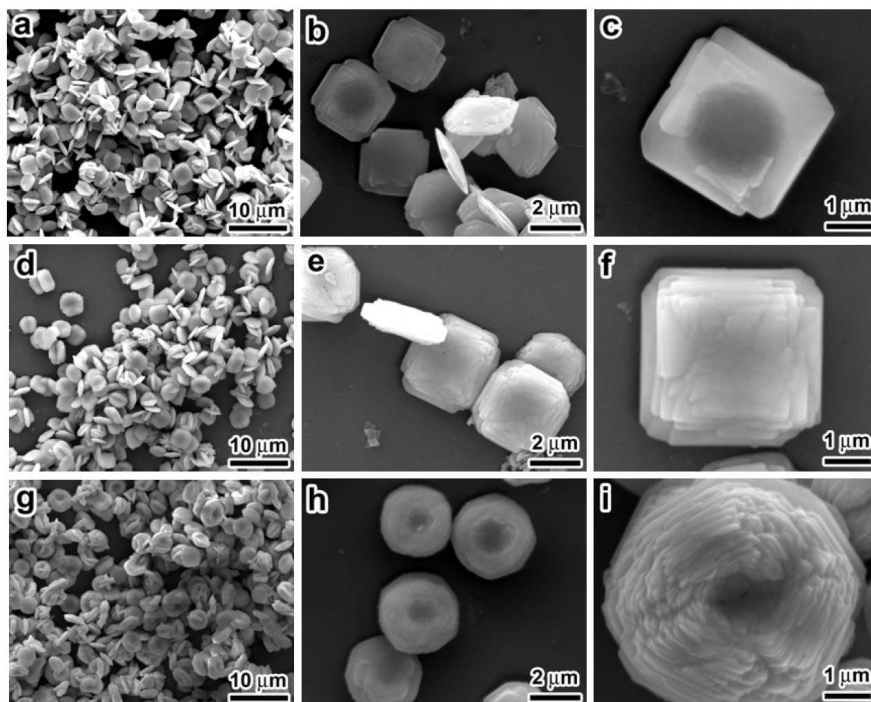


Fig. 4. SEM images of CdMoO_4 samples obtained at 100°C with different concentrations of CdCl_2 aqueous solution. (a-c) 0.02 M , (d-f) 0.04 M and (g-i) 0.2 M .

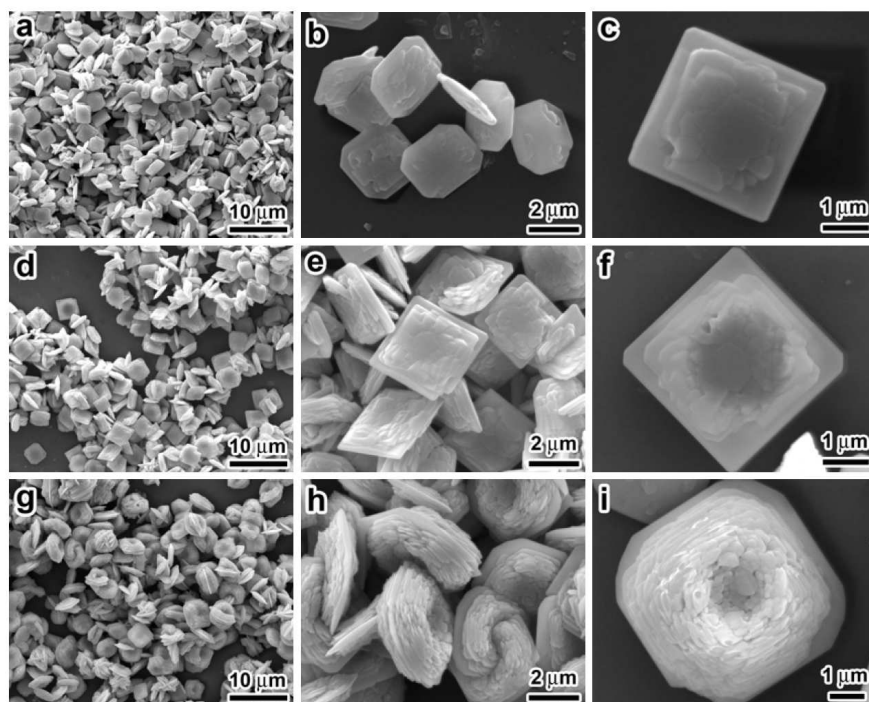


Fig. 5. SEM images of CdMoO_4 samples obtained at 150°C with different concentrations of CdCl_2 aqueous solution. (a-c) 0.02 M, (d-f) 0.04 M and (g-i) 0.2 M.

The following two steps are believed to be responsible for the formation of CdMoO_4 : $(\text{NH}_4)_6\text{Mo}_7\text{O}_{24}^{6-} + 8\text{OH}^- = 7\text{MoO}_4^{2-} + 4\text{H}_2\text{O}$ (Reaction 1), and $\text{Cd}^{2+} + \text{MoO}_4^{2-} = \text{CdMoO}_4$ (Reaction 2). We found that the gradual release of MoO_4^{2-} from $(\text{NH}_4)_6\text{Mo}_7\text{O}_{24}$ is critical to the formation of CdMoO_4 hierarchical structures. Replacing $(\text{NH}_4)_6\text{Mo}_7\text{O}_{24}$ with Na_2MoO_4 (0.2M aqueous solution) as the Mo source while keeping the other reaction conditions the same results in the formation of microspheres with diameters of $\sim 4\ \mu\text{m}$ together with microparticles with sizes of $\sim 1\ \mu\text{m}$ (Fig. S2). The microspheres are constructed by nanoparticles, which is consistent with previous CdMoO_4 microspheres.^{16,20} Comparing the two types of Mo sources, using $(\text{NH}_4)_6\text{Mo}_7\text{O}_{24}$ as the precursor might have the advantage of relatively slow release of MoO_4^{2-} ions so that the reaction kinetics favors the generation of CdMoO_4 hierarchical structures constructed by nanoplates.

According to Reaction 1, the transformation of $\text{Mo}_7\text{O}_{24}^{6-}$ to MoO_4^{2-} ions is strongly pH dependent. Changing the original pH value (~ 5) have serious effects on the morphology of CdMoO_4 products. Decreasing pH value to 4 produces no precipitates since CdMoO_4 is easy to dissolve in acid condition. Increasing pH value to 6, for example, the obtained

sample is composed of plate-like structures with octahedral shape (Fig. S3a,b). Further increasing the pH value results in microspheres (Fig. S3c-f). Similar with our previous case of CaMoO_4 microstructures,⁴ the initial increase of pH apparently promotes the formation of more MoO_4^{2-} and enhances the overall growth rates so that microspheres are finally produced, which is consistent with the results by using Na_2MoO_4 as Mo source (Fig. S2).

To further investigate the formation process of the CdMoO_4 hierarchical structures, the intermediate products obtained with concentration of CdCl_2 aqueous solution at 0.04 M with different precipitation durations were studied in detail by SEM observation. At a short reaction time of 5 min, CdMoO_4 nanoplates with spherical shape and diameter of $\sim 2.5 \mu\text{m}$ are prepared (Fig. 6a and b). Elongating the reaction time to 30 min, CdMoO_4 grow from nanoplates to hierarchical structures and the size increases to $\sim 4 \mu\text{m}$. Small nanoplates are self-constructed on the main nanoplates on both side at this stage (Fig. 6c and d). Further increasing reaction time to 2 hours produces 3D CdMoO_4 hierarchical structures (Fig. 1). Considering both concentration and reaction time dependent change of morphology from single main nanoplates to thick doughnuts, we believe the growth of CdMoO_4 hierarchical structures is similar with our previous CaMoO_4 microstructures with doughnut shape,⁴ which is described by using a model proposed by Sujimoto et al. for the formation of highly uniform peanut-type hematite particles.^{26,28} In our case, CdMoO_4 main nanoplates are formed first with the assistance of NaCl in the reaction system, which are two dimensional anisotropic structures.²⁴ Then, the flat surfaces of main nanoplates serve as nucleation sites for additional small nanoplate growth. Due to the variation in the concentration of precursors, the outer edge of the new nanoplates grows more extensively and becomes relatively thicker than that close to the nucleation sites. This is similar to the formation of truncated core shaped subcrystals at the outer surface of hematite peanuts.^{27,28} Because the surface nucleation rate on the external surfaces is higher than that on the internal surfaces,²⁸ the particles also show considerable growth in the direction perpendicular to the main nanoplates, especially at a high concentration of precursors. Based on the concentration-dependent experiments, we can conclude that the axial growth is preferred at higher concentration of precursors to produce thick hierarchical structures. At high reactant concentrations, the monomer concentration in the solution is higher, which increases the

chemical potential of the system and promotes the growth of the nanoplate building blocks, which tend to stack face-to-face to decrease surface energy by reducing exposed areas, forming thick hierarchical structures.

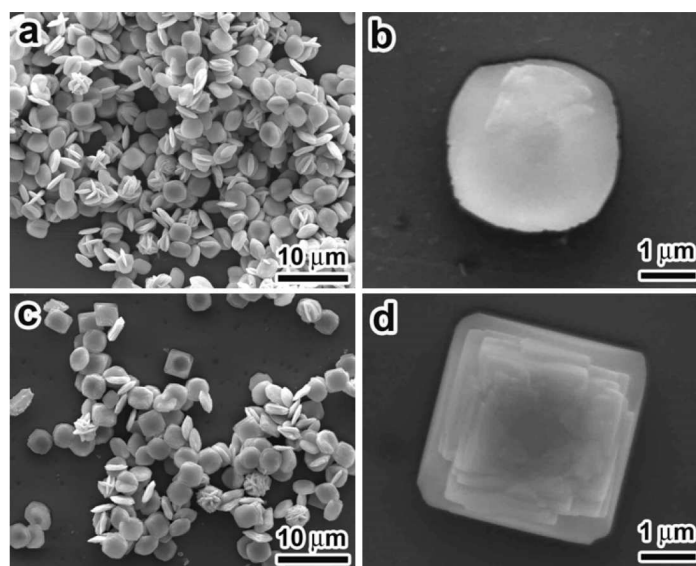


Fig. 6. SEM images of CdMoO₄ samples obtained at different reaction time. (a, b) 5 min and (c, d) 30 min, while keeping the concentration of CdCl₂ aqueous solution at 0.04 M.

Fig. 7a shows the diffuse reflection spectra of CdMoO₄ samples obtained at 200 °C with different concentrations of CdCl₂ aqueous solution. The absorption spectrum of CdMoO₄ shows a strong absorption peak in the wavelength of 230-360 nm, and an absorption edge in 360-450 nm regions. The absorption of CdMoO₄ under UV regions was assigned to the band transition from the occupied O 2p orbital to the empty Mo 4d orbital. For a crystalline semiconductor, the optical absorption near the band edge follows the equation: $\alpha E_{photo} = K(E_{photo} - E_g)^{n/2}$, where α is the absorption coefficient, E_{photo} the discrete photo energy, K a constant, and E_g the band gap energy. Among them, n depends on the characteristics of the transition in a semiconductor, direct transition ($n = 1$) or indirect transition ($n = 4$). For CdMoO₄, the value of n is 1. A classical Tauc approach is further employed to estimate the E_g value of CdMoO₄ hierarchical structures. The intercept of the tangent to the plot gives a good approximation of the band gap energy for indirect band gap materials. **Fig. 7b** displays the plots of $(\alpha E_{photo})^2$ vs E_{photo} based on the direct transition. The value estimated from the intercept of the tangents to the plots was 3.26 eV, which is similar with CdMoO₄ nanostructures reported by Zhou et al.¹⁶ All these samples show the same E_g value since they have a similar structures.

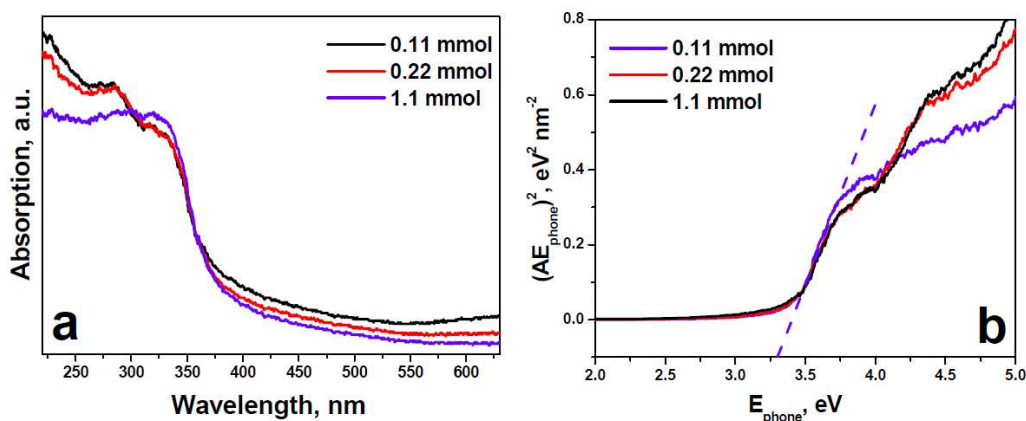


Fig. 7. (a) UV-vis diffuse reflection spectrum and (b) $(\alpha E_{\text{photon}})^2$ vs E_{photon} curves of CdMoO₄ samples obtained with different concentrations of CdCl₂ aqueous solution.

Fig. 8a shows the evolution of RhB absorbance spectra in the presence of the CdMoO₄ hierarchical structures (SEM images are shown in Fig. 1g-i) exposed to UV light for various time periods. The absorption peaks of RhB solution at 553 nm lower down sharply with increasing UV illumination time, indicating that the photocatalytic activity on degradation of RhB by CdMoO₄ hierarchical structures is high. The corresponding plot for the photo-degradation efficiencies of RhB mediated by different photocatalysts under UV light illumination with otherwise identical conditions are shown in Fig. 8b. The blank test demonstrated that the degradation of RhB was extremely slow in the absent of CdMoO₄ (curve i in Fig. 8b), proving the photo-degradation of RhB by CdMoO₄ under UV illumination. For comparison, photo-degradation of RhB by CdMoO₄ nanoplates were also tested.²⁴ The photo-degradation efficiency of RhB by CdMoO₄ nanoplates only reaches 61% after UV illumination time of 60 min (curve ii in Fig. 8b), while 96% of RhB is photo-degraded by CdMoO₄ hierarchical structures within 50 min under UV light illumination (curve iii in Fig. 8b). In addition, the photocatalytic activity of CdMoO₄ hierarchical structures can be further enhanced by calcinating the samples at 500 °C in air for 3 h. The photo-degradation efficiency of RhB by calcined CdMoO₄ hierarchical structures reaches 98% after UV illumination time of 30 min (curve vi in Fig. 8b).

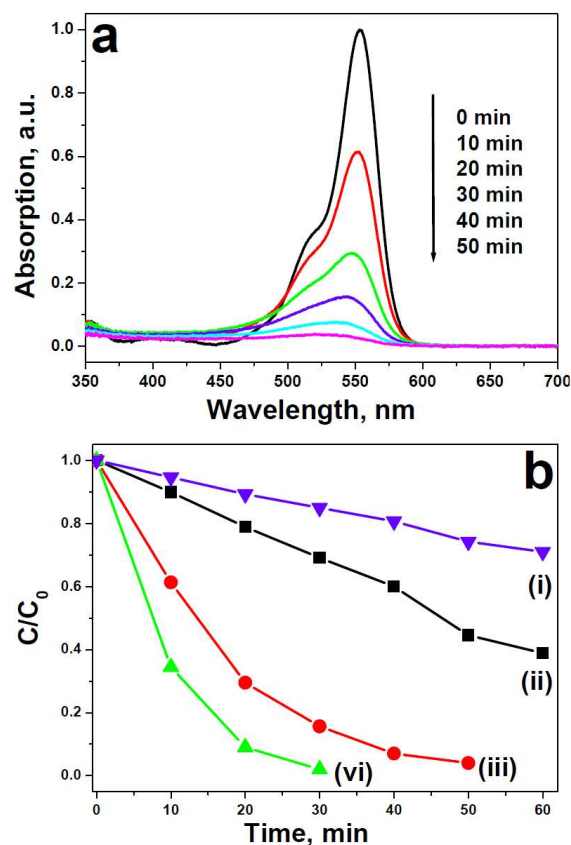


Fig. 8. (a) Absorption spectra of a solution of Rhodamine B in the presence of CdMoO₄ hierarchical structures. (b) Photocatalytic performance of various samples. (i) without CdMoO₄, (ii) CdMoO₄ nanoplates, (iii) CdMoO₄ hierarchical structures, and (vi) calcined CdMoO₄ hierarchical structures.

The above results show that CdMoO₄ hierarchical structures constructed by nanoplates have a higher photocatalytic activity toward photo-degradation of RhB than that of CdMoO₄ nanoplates. It is well known that the photocatalytic activity is dominated by the balance among the photoadsorption, crystallinity, surface area and morphology of the photocatalyst.^{29,30} In the present study, the dark experiment with different CdMoO₄ photocatalyst demonstrated that no significant decrease in the RhB concentration was observed even after 30 minutes, indicating almost no RhB photoadsorption and degradation occurred in the dark (Figure S4). The Brunauer-Emmett-Teller (BET) surface areas of CdMoO₄ hierarchical structures, nanoplates and calcined CdMoO₄ hierarchical structures calculated from N₂ isotherms are 9.45, 42.78 and 11.74 m²/g, respectively. High surface area could increase the number of active sites and help to promote the separation efficiency of the electron-pairs in photocatalytic reactions,

leading to a higher photocatalytic activity. Although the surface areas of CdMoO₄ hierarchical structures are lower than that of CdMoO₄ nanoplates, CdMoO₄ hierarchical structures exhibit a higher crystallinity than CdMoO₄ nanoplates (as revealed by XRD patterns in Figure S5), which implies fewer defects acting as photogenerated electron-hole recombination centers in CdMoO₄ hierarchical structures. In addition, the unique hierarchical structures of CdMoO₄, which consist of numerous nanoplates with preferential orientation, is more favorable for spatial transfer of the photoexcited carriers.³¹⁻³⁶ Furthermore, the hierarchical structures can allow multiple reflections of UV light, which enhances light-harvesting and thus increasing the quantity of photogenerated electrons and holes available to participate in the photocatalytic reaction.²⁹ Consistent with our previous study demonstrated that calcination of CdMoO₄ samples can further improve the crystallinity (Figure S5), which is the most important factor that affects photocatalytic activity since the lattice defects may act as recombination centers for the photoinduced electrons and holes, reducing significantly the net photocatalytic activity.³⁷

4. Conclusions

In conclusion, a facile sodium chloride assisted hydrothermal route was developed to synthesize CdMoO₄ hierarchical structures constructed by numerous single-crystalline nanoplates. The size and morphology of can be tuned CdMoO₄ hierarchical structures by controlling the reaction conditions. The two-step growth was proposed for the formation mechanism of CdMoO₄ hierarchical structures, in which CdMoO₄ main nanoplates were formed first in the synthesis, followed by self-construction of small nanoplates on both side of the main nanoplates in a regular fashion. The photocatalytic activities of CdMoO₄ hierarchical structures were evaluated by the degradation of RhB under UV light illumination. Due to the unique morphology and high crystallinity, CdMoO₄ hierarchical structures exhibited better activity performance than nanoplates.

Acknowledgment. This work was financially supported by National Natural Science Foundation of China (No. 51102065 and 51371072), the Fundamental Research Funds for the Central Universities (Grant No. HIT. NSRIF. 2010114), Specialized Research Fund for the Doctoral Program of Higher Education (SRFDP. 20112302120019). W.S.W. thanks

support from Heilongjiang Province Postdoctoral Fellowships and China Postdoctoral Science Foundation (No. 20110491039, and 2012T50329).

References

1. B. Wang, H. B. Wu, L. Yu, X. W. Lou, *Adv. Mater.* 2012, **24**, 1111.
2. B. Wang, H. B. Wu, L. Zhang, X. W. Lou, *Angew. Chem. Int. Ed.* 2013, **52**, 4165.
3. W. S. Wang, L. Zhen, C. Y. Xu, W. Z. Shao, *CrystEngComm* 2011, **13**, 625.
4. W. S. Wang, Y. X. Hu, J. Goebel, Z. D. Lu, L. Zhen, Y. D. Yin, *J. Phys. Chem. C.* 2009, **113**, 16416.
5. B. Zou, Y. Liu, Y. Wang, *RSC Adv.* 2013, **3**, 23327.
6. W. Lee, J. Yi, S. Kim, Y. Kim, H. Park, W. Park, *Cryst. Growth Des.* 2011, **11**, 4927.
7. Z. Sun, J. Kim, Y. Zhao, F. Bijarbooneh, V. Malgras, Y. Lee, Y. Kang, S. Dou, *J. Am. Chem. Soc.* 2011, **133**, 19314.
8. H. Yuan, W. Ma, C. Cheng, H. Zhu, X. Gao, J. Zhao, *J. Phys. Chem. C* 2011, **115**, 23256.
9. T. Lin, C. Lin, H. Liu, J. Sheu, W. Hung, *Chem. Commun.* 2011, **47**, 2044.
10. M. R. Alenezi, S. J. Henley, N. G. Emerson, S. R. P. Silva, *Nanoscale* 2014, **6**, 235.
11. G. Zhu, C. Xi, H. Xu, D. Zheng, Y. Liu, X. Xu, X. Shen, *RSC Adv.* 2012, **2**, 4236.
12. Q. Wang, L. Jiao, H. Du, W. Peng, Y. Han, D. Song, Y. Si, Y. Wang, H. Yuan, *J. Mater. Chem.* 2011, **21**, 327.
13. L. Zheng, Y. Xu, Y. Song, C. Wu, M. Zhang, Y. Xie, *Inorg. Chem.* 2009, **48**, 4003.
14. V. B. Mikhailik, H. Kraus, D. Wahl, M. S. Mykhaylyk, *Phys. Stat. Sol. B* 2005, **242**, R17.
15. A. Jayaraman, S. Y. Wang, S. K. Sharma, *Phys. Rev. B* 1995, **52**, 9886.
16. L. Zhou, W. Wang, H. Xu, S. Sun, *Cryst. Growth Des.* 2008, **8**, 3595.
17. W. Wang, L. Zhen, C. Xu, B. Zhang, W. Shao, *J. Phys. Chem. B* 2006, **110**, 23154.
18. W. Wang, L. Zhen, C. Xu, W. Shao, *Cryst. Growth Des.* 2009, **9**, 1558.
19. W. Wang, L. Zhen, C. Xu, W. Shao, Z. Chen, *CrystEngComm.* 2013, **15**, 8014.
20. D. Li, Y. Zhu, *CrystEngComm* 2012, **14**, 1128.
21. Q. Gong, G. Li, X. Qian, H. Cao, W. Du, X. Ma, *J. Colloid Interface Sci.* 2006, **304**, 408.
22. L. Hou, L. Lian, L. Zhang, J. Li, *Mater. Lett.* 2013, **109**, 306.
23. G. Xing, Y. Xu, C. Zhao, Y. Wang, Y. Li, Z. Wu, T. Liu, G. Wu, *Powder Technol.* 2011, **213**, 109.

24. W. Wang, L. Zhen, W. Shao, Z. Chen, *Mater. Lett.* 2014, **313**, 292.
- 25 Y. Chen, M. Wen, Q. Wu, *CrystEngComm*. 2011, **13**, 3035.
- 26 T. Sugimoto, M. Khan, A. Muramatsu, H. Ito, *Colloids Surf. A* 1993, **79**, 233.
- 27 D. Shindo, G. Park, Y. Waseda, T. Sugimoto, *J. Colloid Interface Sci.* 1994, **168**, 478.
- 28 N. Sasaki, Y. Murakami, D. Shindo, T. Sugimoto, *J. Colloid Interface Sci.* 1999, **213**, 121.
- 29 H. Li, Z. Bai, J. Zhu, D. Zhang, G. Li, Y. Huo, H. Li, Y. Lu, *J. Am. Chem. Soc.* 2007, **129**, 8406.
- 30 F. Liu, W. Cai, Y. Zhang, *Adv. Funct. Mater.* 2008, **18**, 1047.
- 31 H. Cheng, B. Huang, Z. Wang, X. Qin, X. Zhang, Y. Dai, *Chem. Eur. J.* 2011, **17**, 8039.
- 32 L. Xu, X. Yang, Z. Zhai, W. Hou, *CrystEngComm*. 2011, **13**, 7267.
- 33 J. Yu, Y. Su, B. Cheng, *Adv. Funct. Mater.* 2007, **17**, 1984.
- 34 Y. Li, G. Duan, G. Liu, W. Cai, *Chem. Soc. Rev.* 2013, **42**, 3614.
- 35 Y. Li, T. Sasaki, Y. Shimizu, N. Koshizaki, *Small* 2008, **4**, 2286.
- 36 Y. Li, N. Koshizaki, H. Wang, Y. Shimizu, *ACS Nano* 2011, **5**, 9403.
- 37 L. Zhen, W. Wang, C. Xu, W. Shao, Z. Chen, *Scripta Mater.* 2008, **58**, 461.

TOC:

